express
polymer letters

Research article

Fully bio-based poly(butylene succinate-*co*-butylene 2,5-thiophenedicarboxylate) with derived from 2,5-thiophenedicarboxylic acid

Guoqiang Wang[*] [iD], *Xingyu Hao, Yakun Dong, Li Zhang, Rubo Sun*

College of Material Science and Engineering, Jilin Jianzhu University, 130118 Changchun, China

Abstract. Novel poly(butylene succinate-*co*-butylene 2,5-thiophenedicarboxylate) (PBSTFs) were successfully synthesized by changing the ratio of 2,5-thiophenedicarboxylic acid (TDCA) and 1,4-succinic acid (SA) through two-step melt polycondensation. Their structure, thermal properties, crystalline properties, mechanical properties, and rheological properties were tested and characterized. The glass transition temperature increases with the increase of butylene 2,5-thiophenedicarboxylate unit (BTF). NMR results show that the copolymers are random copolymers. Differential scanning calorimetry (DSC) and wide-angle X-ray diffraction (WAXD) results show that all polyesters are semi-crystalline polymers. When the content of TDCA is 0–50%, the crystallinity and melting temperature of the samples decreased, Young's modulus and tensile strength decreased, and the elongation at break increased obviously with the increase of BTF. When the content of TDCA is 50–100%, the tensile strength increases, but the elongation at break decreases slightly. The range of strength is between 15.4 and 38 MPa, and the maximum elongation at break can reach 1160%. Therefore, by adjusting the content of BTF, the structure of copolyesters can be adjusted to obtain fully bio-based copolyesters with excellent properties. Compared with poly(butylene succinate), when the molar percentage of TDCA in a product is 29%, the copolyester has better mechanical properties (tensile strength: 31.4 MPa and elongation at break: 1060%), higher glass transition temperature (–26.2 °C) and better processing properties.

Keywords: material testing, 2,5-thiophenedicarboxylic acid (TDCA), poly(butylene succinate) (PBS), bio-based polyesters

1. Introduction

With the overexploitation and utilization of traditional petrochemical resources all over the world, the petrochemical industry has become an indispensable part of human daily life and production. However, in recent years, due to the large-scale development of petrochemical resources, atmospheric warming and environmental pollution, including air pollution caused by incineration, soil pollution caused by landfills, marine pollution caused by inflow and atomization, in order to reduce the development of non-renewable petrochemical resources, many experts began to pay attention to the development of alternative traditional petroleum resources. Therefore, renewable and biodegradable bio-based resources have attracted more and more academic attention [1–5].

In recent years, a large number of bio-based polyesters have been developed successively, such as polylactic acid (PLA) [6], poly(propanediol fumarate) (PPF) [7], poly(butanediol succinate) (PBS) [8] and so on. The rapid development of the conversion and utilization of biomass resources has brought opportunities to the synthesis of bio-based monomers and bio-based polyesters. PBS is widely used because of its excellent properties and relatively low

price. PBS is a kind of semi-crystalline aliphatic polyester, which has good melting processing properties, mechanical properties, heat resistance, and degradation properties, and the use of PBS meets the requirements of national sustainable development [9–12]. However, barrier properties of PBS are poor and tensile strength, impact toughness, and glass transition temperature are low, so copolymerization and blend are often used to improve various properties of PBS [13–17].

In order to improve the glass transition temperature and toughness of PBS, Luo *et al.* [18] synthesized poly(butylene succinate-*co*-butylene terephthalate) (PBSTs) by direct esterification, and the melting temperature, glass transition temperature, storage modulus, and loss modulus of the copolyesters were characterized. The results showed that they were positively correlated with the butylene terephthalate unit (BT). Young's modulus and tensile strength at break of copolyesters with higher BT content were also higher, but the elongation at break was lower. PBSTs showed high melting temperature (139.6–179.4 °C) and tensile toughness (elongation at break >400%) when the content of BT unit was 40–60%. However, terephthalic acid mainly comes from petroleum. In order to improve the glass transition temperature and toughness of PBS by using bio-based monomers, Wu *et al.* [17] synthesized poly(butylene succinate-butylene fumarate) (PBSFs) copolyesters with full component content through direct esterification polycondensation. For PBSFs, Young's modulus is 360–1800 MPa, and tensile strength is 20–35 MPa, elongation at break is 2.5–660%. The tensile strength of PBS is 30 MPa, elongation at break is 130%, and glass transition temperature is –40 °C. Compared with PBS, PBSF60 showed higher glass transition temperature (6.5 °C) and toughness (elongation at break ~660%) when butylene furandicarboxylate unit content is 60%. However, the melting temperature of PBSF60 (111 °C) is equivalent to that of PBS (115 °C). At the same time, PBSF60 shows excellent biodegradability [19]. Copolymerization often reduces the crystallinity of PBS, which leads to better toughness, but the strength often decreases. In order to improve the strength and toughness of PBS at the same time, Kim *et al.* [3] successfully synthesized poly(butylene succinate-*co*-butylene carbonate) (PBSC) nanocomposites with citric acid and cellulose nanocrystals (CNCs), which further improved tensile strength, tensile toughness and tear toughness

of PBS. The introduction of dimethyl carbonate (DMC) destroys the regularity of PBS chain and reduces the crystallinity. Therefore, the toughness of PBSC becomes better. Citric acid as a chemical crosslinking agent and cellulose nanocrystals as a physical crosslinking agent were added to improve tensile strength. PBSC nanocomposite with a tensile strength of 64 MPa, tear strength of 1.4 kN/cm, tear toughness of 32 J/cm, and elongation at break of 690% was obtained.

Hong *et al.* [20] enhanced PBS with bamboo fiber modified by triethoxysilane and polydopamine (PDA), and its performance was greatly improved. The tensile strength, tensile modulus, bending strength, bending modulus, and impact strength were increased by 70, 25, 37, 24, and 63%, respectively. The degradation rate of PBS is slow due to the high crystallinity of PBS. In order to improve the degradation properties and toughness of PBS, Hu *et al.* [21] successfully synthesized poly(butylene succinate-*co*-glycolate) (PBSGA) copolyester with 5–40% glycolic acid (GA) content. It was found that the addition of GA hindered the crystallization of PBS, resulting in an increase in hydrophilicity and accelerated degradation rate. PBSGA30 showed higher elongation at break (1150%) when the content of the glycolate unit was 60%. At the same time, PBSGA30 shows the tensile strength (30.0 MPa) equivalent to PBS. However, the barrier properties did not increase as expected but decreased. In order to improve glass transition temperature and barrier properties of PBS, Wang *et al.* [22] synthesized PBS-based copolyesters with isosorbide (IS) or 2,3-O-isopropylidene-Lthreitol (ITh), and studied the effects of Is or ITh on the tensile strength, elongation at break and oxygen properties of PBS. The results showed that the crystallinity and crystallization rate of PBS decreased, the glass transition temperature increased, and the hydrophilicity was improved. Compared with PBS, the barrier property of copolyester has been improved to a certain extent. Meanwhile, the oxygen barrier property and mechanical properties of the double ring IS-based copolyesters were better than those of the single ring Ith-based copolyesters.

At present, 2, 5-thiophenedicarboxylic acid (TDCA) and 2,5-furandicarboxylic acid (FDCA) are the most studied bio-based monomers. There are many reports on FDCA-based copolyesters or homopolyesters, such as poly(ethylene furandicarboxylate) (PEF)

[23], poly(propylene furandicarboxylate) (PPF) [24], poly(butene furandicarboxylate) (PBF) [25], poly(butadiene adipate-*co*-butadiene furandicarboxylate) (PBAFs) [26], and poly(butadiene succinate-*co*- butadiene furandicarboxylate) (PBSFs) [17]. TDCA can also be synthesized from biomass, and some TDCA-based copolyesters have been successfully synthesized [27–29]. However, there are few reports on PBS-based copolyesters containing TDCA.

In this paper, to improve the toughness and glass transition temperature of PBS with the cheap bio-based monomer, poly(butylene succinate) (PBS), poly(butylene 2,5-thiophenedicarboxylate) (PBTF), and poly(butylene succinate-*co*-butylene 2,5-thiophenedicarboxylate) (PBSTFs) with different TDCA contents were successfully synthesized by direct esterification and melt polycondensation. The microstructures, crystallization properties, thermal properties, and mechanical properties were characterized.

2. Experiments
2.1. Materials
1,4-Succinic acid (SA, 99%) was purchased from Nanjing Kangmanlin Chemical Industry Co., Ltd. (Nanjing, China). 1,4-Butanediol (BDO, 99%) and tetrabutyl titanate (TBT, 99%) were purchased from Shanghai Aladdin Biochemical Technology Co., Ltd. (Shanghai, China). 2,5-Thiophenedicarboxylic acid (TDCA, >99%) was purchased from Innochem Co., Ltd. (Beijing, China).

2.2. Synthesis of PBS, PBTF, and PBSTFs
PBS, PBTF, and PBSTFs were synthesized by esterification and polycondensation reaction. In the first stage, BDO, TBT, and SA/TDCA were added to the reactor equipped with the mechanical stirrer at 170 rpm. For PBS and PBSTFs, the total content of the diacid (SA+TDCA) was 0.25 mol. For PBTF, the content of TDCA was 0.2 mol. The molar ratio of diol to diacid was 3:1, and the content of TBT was 30 μl/mol diacid. The reactor was heated to 190 °C under N$_2$ atmosphere for 4 h. Subsequently, in the second stage, the reactor was heated to 230 °C under vacuum for polycondensation reaction, and the polycondensation reaction stopped when the rod climbing phenomenon occurred. The copolymers are named PBSTFφ_{BTF}, where φ_{BTF} [%] is the molar percentage of butylene 2,5-thiophenedicarboxylate unit in copolymers. PBS, PBTF, PBSTF48, and PBSTF73 were synthesized by the above method.

For PBSTF29, we adopted the following procedure: for the esterification reaction, SA, BDO, and TBT were placed in one reactor, and TDCA, BDO, and TBT were placed in another reactor. The esterification reaction was also carried out at 190 °C under N$_2$ atmosphere for 4 h. After the esterification, the above mixtures were added to the same reactor for polycondensation. The reactor was heated to 230 °C under vacuum for polycondensation reaction, and the polycondensation reaction stopped when the rod climbing phenomenon occurred.

2.3. Characterization
Gel permeation chromatography (GPC)
The molecular weights of PBS, PBTF, and PBSTFs were determined at 30 °C by gel permeation chromatography (Waters 1515, USA). Chloroform was used as eluent and polystyrene as standard for calibration.

Fourier transform infrared spectroscopy (FTIR)
Firstly, PBS, PBTF, and PBSTFs were pressed into a film at 150–180 °C and then pressed at room temperature. FTIR spectra were recorded using a Thermo Nicolet IS50 FT-IR spectrometer (USA) at a resolution of 4 cm^{-1} and 32 scans for each spectrum. The films were tested with a scanning range of 650~4000 cm^{-1}.

Nuclear magnetic resonance
The solvent was deuterium chloroform (CDCl$_3$). 5–10 mg sample is dissolved in 0.5 ml CDCl$_3$. ^{1}H NMR spectra were measured by 600 MHz Bruker Avance system (Germany).

Differential scanning calorimetry (DSC)
Differential scanning calorimetry (DSC) curves were recorded using a TA DSC Q20 instrument (TA Instruments, USA). 5~10 mg samples were weighed and tested in N$_2$ atmosphere at 50 ml/min. First, the sample was heated from –60 to 200 °C at the rate of 10 °C/min. The temperature was held at 200 °C for 3 min, and then the sample was cooled from 200 to –60 °C at the rate of 10 °C/min. Finally, the sample was heated from –60 to 200 °C at the rate of 10 °C/min.

Thermogravimetric analysis (TGA)
Thermogravimetric analysis (TGA) curves were recorded using a TA TGA Q50 instrument (TA Instruments, USA). 3~5 mg samples were weighed in

N$_2$ atmosphere of 50 ml/min at a heating rate of 10 °C/min and a temperature range of 50–600 °C.

Wide-angle X-ray diffraction (WAXD): X-ray diffraction (XRD) spectra were recorded on the Ultima IV 2036E102 spectrometer (Japan) and Bruker D8 ADVANCE X-ray diffractometer (Germany). X-ray diffraction profile was obtained at a scanning speed of 5°/min. The scanning range was 5–45°.

Tensile test: PBS, PBTF, and PBSTF were hotpressed into sheets at 150–180 °C using 0.5 mm thick iron sheets and then pressed at room temperature. Finally, they were made into dumbbell tensile specimens using a cutting knife according to GB/T 528. The tensile properties were measured at room temperature with an Instron 3365 tester (USA) at a tensile speed of 50 mm/min. Five specimens were tested, and the tensile-related data are shown in Table 4.

Rheological properties: Rheological properties of PBS, PBTF, and PBSTFs were characterized using a TA DHR-2 rheometer (TA Instruments, USA) with a parallel plate geometry in an oscillation model under nitrogen. The test conditions are as follows: an angular frequency of 10 rad/s, a strain of 1.25% and a heating rate of 3 °C/min.

3. Results and discussion
3.1. Synthesis and chemical structures of PBS, PBTF, and PBSTFs

Bio-based copolymers were synthesized from BDO, SA, and TDCA through a two-step esterification polycondensation reaction as shown in Figure 1.

For the synthesis of PBS and PBTF, the ratio of diacid to diol was 1:3, and TBT was used as a reaction catalyst at 190 °C in N$_2$ atmosphere to successfully synthesize PBS and PBTF with high molecular weight, indicating that esterification reaction is easy to occur, and TDCA and SA can be well esterification reaction with BDO. Under the same conditions, PBSTF48 and PBSTF73 with high molecular weight were also obtained. However, PBSTF29 synthesized by the above method was brittle, indicating the molecular weight was not high enough. The reasons may be as follows: the strong acidity of TDCA leads to the cyclization of BDO to tetrahydrofuran, and SA with weak acidity reacts slowly with BDO, resulting in incomplete esterification of SA with BDO for PBSTF29. In order to successfully synthesize PBSTF29 with high molecular weight, the following procedure was adopted: for the esterification reaction, SA, BDO, and
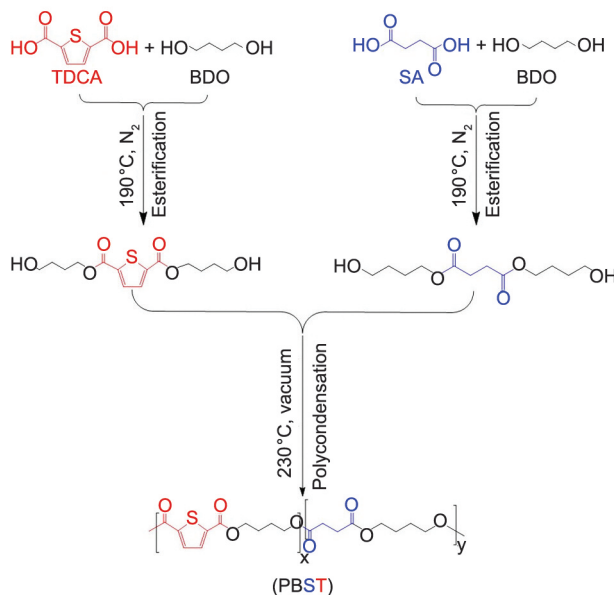

Figure 1. Synthesis of PBS, PBTF, and PBSTF from BDO, SA and TDCA.

TBT were placed in one reactor, and TDCA, BDO, and TBT were placed in another reactor. The esterification reaction was also carried out at 190 °C under N$_2$ atmosphere for 4 h. After the esterification, the above mixtures were added to the same reactor for polycondensation. The reactor was heated to 230 °C under vacuum for polycondensation reaction, and the polycondensation reaction stopped when the rod climbing phenomenon occurred. Through this method, PBSTF29 with high molecular weight was successfully synthesized. In fact, in the esterification stage, BDO was converted to tetrahydrofuran (THF), and THF was distilled with water. It was also mentioned in the previous report that there was a small amount of THF in the reaction of SA and BDO [30]. Wu *et al.* [17] also explained the phenomenon in their study. The presence of FDCA in the reaction catalyzed the generation of side reactions, and the content of THF increased with the increase of the content of FDCA. The chemical structures of PBS, PBTF, and PBSTFs were analyzed by FTIR and 1H NMR. FTIR spectra of PBS, PBSTFs, and PBTF are shown in Figure 2. The region between 3000–2700 cm^{-1} is the C–H stretching vibration region, and it is the C–H stretching vibration on saturated carbon. An obvious absorption peak (I) appears in the region of 1755–1670 cm^{-1}, which is the stretching vibration region of the carbonyl group. Due to the large electric dipole moment of the carbonyl group, the absorption peak is generally strong in FTIR. It can be seen from Figure 2 that all polyesters showed absorption peaks
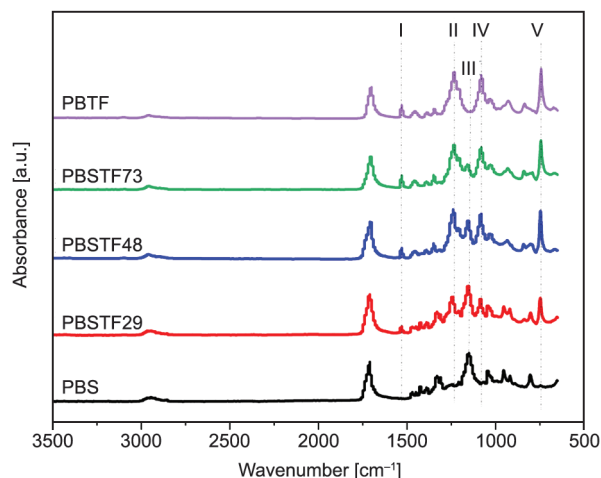
Figure 2. FTIR spectra of PBS, PBTF and PBSTFs.

Figure 3. Chemical structures of SBS, TFBTF and SBTF units in PBS, PBTF, and PBSTFs.

of the ester group, indicating PBS, PBTF, and PBSTFs were synthesized. For PBS, C=O appeared at 1710 cm^{-1}, and for PBTF, it gradually shifted to 1700 cm^{-1}. C=C in thiophene ring can be found at about 1530 cm^{-1} in region II, and its peak gradually increases with the increase of TDCA content. In the 1460-1160 cm^{-1} region, this region mainly includes in-plane bending vibration of C–H, stretching vibration of C–O, and skeleton vibration of C–C. The peak at 1240 cm^{-1} (III) belongs to the stretching vibration of C–-O in the butylene 2,5-thiophenedicarboxylate unit (BTF). The peak at 1160 cm^{-1} (IV) belongs to the stretching vibration peak of C–O in the butylene succinate unit (BS). The peak at 1080 cm^{-1} (V) is the stretching vibration peak of C–S–C in the thiophene ring. The peaks at 834 cm^{-1} (VI) and 742 cm^{-1} (VII) are the bending vibrations of the thiophene ring. With the increase of TDCA content, the intensity of five peaks (II, III, V, VI, and VII) increases and the intensity of Peak IV decreases.

The attributes of chemical shifts are shown in Figure 3, and ^{1}H NMR spectra of PBS, PBSTFs, and PBTF are shown in Figure 4. The results showed that the synthesized polyester had almost no impurity peaks. For PBS, the chemical shift of CH$_2$ in SA unit was at 2.64 ppm (**s**), and the chemical shifts of BDO unit were at 4.13 ppm (**a$_1$**) and 1.72 ppm (**b$_1$**). For PBSTFs, the chemical shifts of **s**, **a$_1$**, and **b$_1$** are retained. Meanwhile, some new chemical shifts appear: the chemical shift of CH in the thiophene ring is 7.75 ppm (**t**), the chemical shift of CH$_2$–C=O in BDO unit is 4.17 ppm (**a$_2$**), 4.36 ppm (**a$_3$**), 4.40 ppm (**a$_4$**), and the chemical shifts of CH$_2$–CH$_2$–C=O in BDO unit are 1.80 ppm (**b$_2$**), 1.85 ppm (**b$_3$**) and 1.94 ppm (**b$_4$**) due to the introduction of TDCA. For PBTF, only chemical

shifts (**t**, **a$_4$**, and **b$_4$**) are included. In addition, with the increase of TDCA content, the intensity of **s**, **a$_1$**, and **b$_1$** decreases, while the intensity of **t**, **a$_4$**, and **b$_4$** increases.

The molar percentage of TDCA in product (Φ_{BTF}), the average sequence length ($L_{n, BS}$ and $L_{n, BTF}$) and random degree (R) of the copolymers were calculated according to ^{1}H NMR spectra. The Equations (1)–(4) were used for calculating the revelent parameters [31]:

$$\Phi_{BTF} \, [\text{mol\%}] = \frac{2I_t}{2I_t + I_s} \cdot 100 \tag{1}$$

$$L_{n, BS} = 1 + \frac{2I_{a_1}}{I_{a_2} + I_{a_3}} \tag{2}$$

$$L_{n, BTF} = 1 + \frac{2I_{a_4}}{I_{a_2} + I_{a_3}} \tag{3}$$

$$R = \frac{1}{L_{n, BS}} + \frac{1}{L_{n, BTF}} \tag{4}$$

where the integral of peak **t**, **s**, **a$_1$**, **a$_2$**, **a$_3$**, and **a$_4$** is abbreviated as I_t, I_s, I_{a_1}, I_{a_2}, I_{a_3}, and I_{a_4}, respectively. The calculated average sequence length and randomness are listed in Table 1. It can be seen that the molar percentage of TDCA in feed is almost identical to the molar percentage of TDCA in the product. With the increase of Φ_{BTF} in feed, $L_{n, BS}$ decreases, and $L_{n, BTF}$ increases, and the sequence length is almost 2 when Φ_{BTF} in feed is 50 mol%. Previous research shows that copolyesters with the average sequence length of aliphatic-aromatic unit <2 are biodegradable [32]. The random degree is about 1, indicating that copolyesters are copolymers with random structures. According to the results of FTIR and ^{1}H NMR
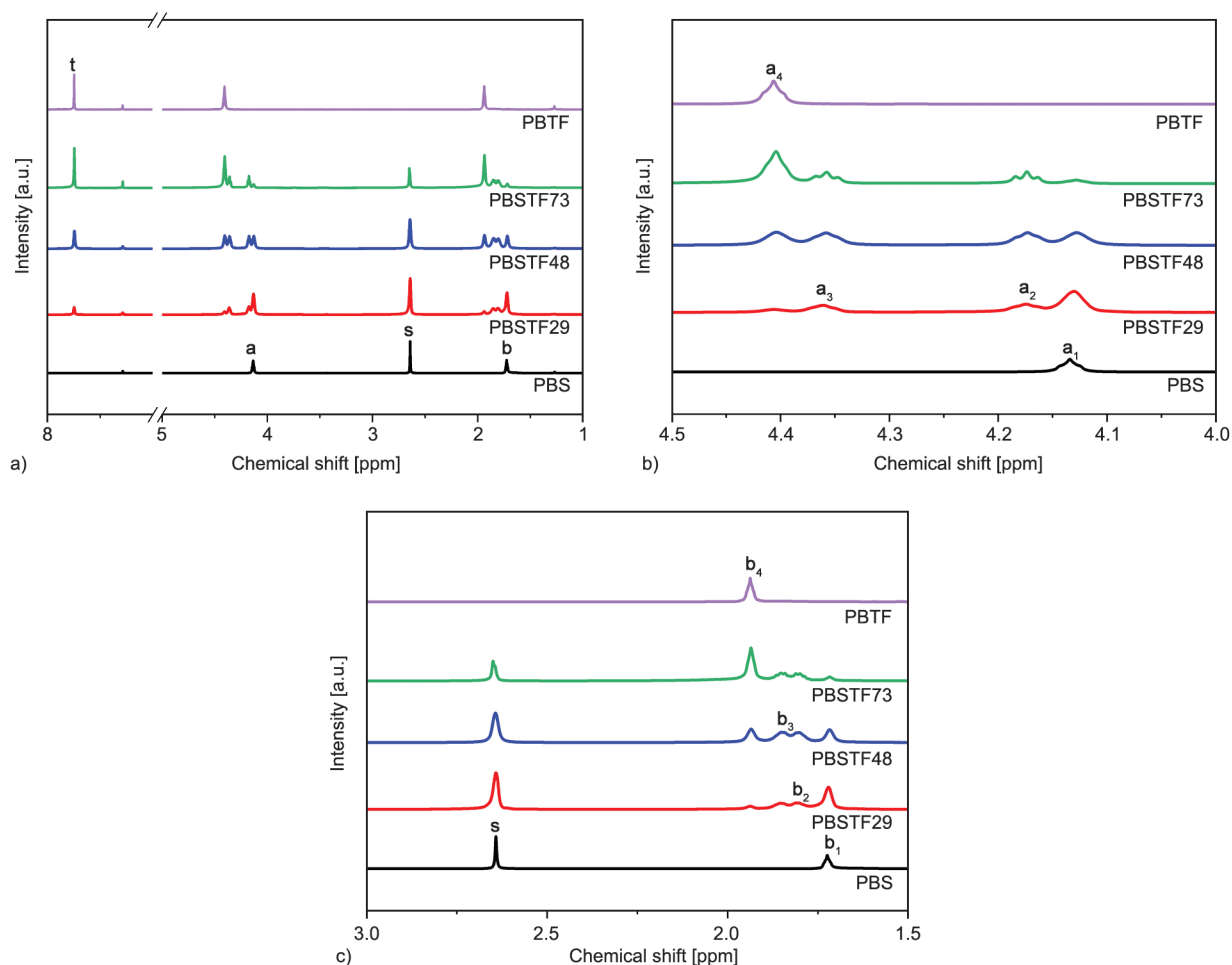
Figure 4. ^{1}H NMR spectra of PBS, PBTF and PBSTFs (a) the whole spectra; (b) and (c) magnification of chemical shifts **a** and **b**.

Table 1. Microstructures and molecular weight of PBS, PBTF and PBSTFs.

Sample	Φ_{BTF} in feed [mol%]	^{1}H NMR	^{1}H NMR			M_w [g/mol]	PDI [–]
		Φ_{BTF} in product [mol%]	$L_{n, BS}$ [–]	$L_{n, BTF}$ [–]	R [–]		
PBS	0	0	–	–	–	69400	2.2
PBSTF29	25	29	3.38	1.32	1.05	42300	2.0
PBSTF48	50	48	1.84	1.88	1.08	33600	1.9
PBSTF73	75	73	1.28	3.58	1.06	29400	2.1
PBTF	100	100	–	–	–	37500	2.0

spectra, we have successfully synthesized PBSTFs with the expected chemical structure.

3.2. Thermal transition behaviors and thermal stability of PBS, PBSTFs, and PBTF

DSC curves of PBS, PBSTFs, and PBTF are shown in Figure 5, and thermal transition data are summarized in Table 2. The thermal transformation behavior and melt crystallization behavior of copolyesters directly affect the physical properties, processing properties, and application of copolyesters. The melting crystallization temperature (T_c) and enthalpy (ΔH_c) were obtained in the cooling scan. The glass transition temperature (T_g), the melting temperature (T_m) and melting enthalpy (ΔH_m), cold crystallization temperature (T_{cc}), and cold crystallization enthalpy (ΔH_{cc}) of PBS, PBTF, and PBSTFs were obtained by DSC in the second heating.

The thermal transformation behavior of PBSTFs is strongly dependent on its components. T_m, ΔH_m, T_c, and ΔH_c of PBSTFs with butylene succinate-rich unit decrease with the increase of ΦBTF, and then T_m, ΔH_m, T_c, and ΔH_c of PBSTFs with butylene
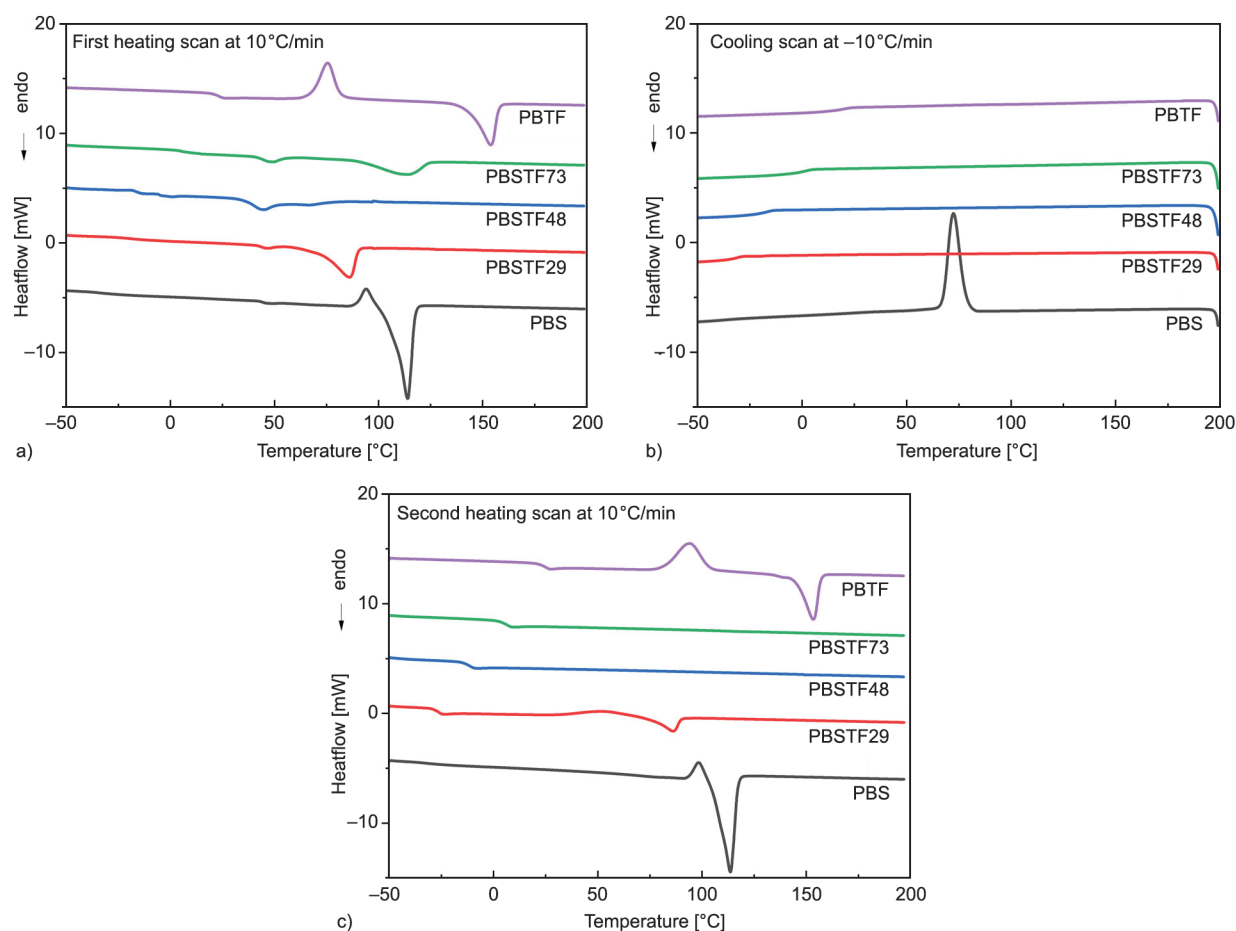
Figure 5. DSC curves of PBS, PBTF and PBSTFs. a) First heating scan, b) cooling scan, c) second heating scan.

2,5-thiophenedicarboxylate-rich unit increase with the further increase of Φ_{BTF}. PBS is a typical crystalline polymer. During the first heating process, PBS exhibits a strong melting peak at 114.0 °C ($\Delta H_{m_1} = 57.5$ J/g). PBS exhibits good crystallization ability during cooling and second heating process. There is high melting crystallization enthalpy at 72.4 °C ($\Delta H_c = 55.2$ J/g) in the cooling scan and high melting enthalpy at 113.6 °C ($\Delta H_m = 55.9$ J/g) in the second heating scan. However, with the addition of TDCA, PBSTFs did not show obvious melt crystallization behavior, indicating that the addition of

TDCA inhibited the crystallization ability of PBS and reduced the crystallization rate and melt crystallization ability of PBSTFs.

For the first heating scan, PBTF showed obvious melting peaks and cold crystallization peaks, but all copolyesters showed only melting peaks. During the second heating scan, PBSTF29 showed a melting peak and cold crystallization peak, while PBSTF48 and PBSTF73 showed no melting peaks and cold crystallization peaks, indicating the crystallization ability of copolyesters was very poor, but under natural cooling conditions, they can still crystallize

Table 2. Thermal properties of PBS, PBTF, and PBSTFs obtained by DSC.

Sample	1st heating							Cooling		2nd heating				
	T_{m_1}[a] [°C]	ΔH_{m_1} [J/g]	T_{m_2}[b] [°C]	ΔH_{m_2} [J/g]	$\Delta H_{m_1} + \Delta H_{m_2}$ [J/g]	T_{cc} [°C]	ΔH_{cc} [J/g]	T_c [°C]	ΔH_c [J/g]	T_g [°C]	T_m [°C]	ΔH_m [J/g]	T_{cc} [°C]	ΔH_{cc} [J/g]
PBS	114.0	57.5	–	–	57.5	94.1	9.4	72.4	55.2	–	113.6	55.9	98.5	7.0
PBSTF29	46.6	1.2	86.1	30.2	31.4	–	–	–	–	–26.2	86.3	10.9	52.7	5.8
PBSTF48	43.9	–	67.7	–	14.9	–	–	–	–	–11.4	–	–	–	–
PBSTF73	49.0	2.8	114.0	16.2	19.0	–	–	–	–	6.5	–	–	–	–
PBTF	154.0	25.9	–	–	25.9	75.6	19.7	–	–	25.0	153.4	23.5	94.3	23.1

[a]T_{m_1}: the first melting peak in the heating scan.
[b]T_{m_2}: the second melting peak in the heating scan.

slowly. Therefore, in the first heating scan, they have obvious melting peaks at 86.1 °C ($\Delta H_{m_2} = 30.2$ J/g), 67.7 °C ($\Delta H_{m_1} + \Delta H_{m_2} = 14.9$ J/g) and 114.0 °C ($\Delta H_{m_2} = 16.2$ J/g), respectively. For PBSTF29, PBSTF48, and PBSTF73, there are two melting peaks. For PBS, an exothermic peak is observed just before melting in the first and second heating scans, so it is more likely a crystal ordering. The crystallization of PBS during cooling is complete (one peak is visible, which has onset and endset), meaning that in the second heating, cold crystallization should not appear. However, there is still an exothermic peak just before melting. The above results confirm that the exothermic peak is not cold-crystallization but a crystal ordering.

Compared with PBS, the melting enthalpy of copolymer decreased. With the increase of TDCA, the ΔH_m of PBSTFs increases first and then decreases, which may be caused by the isodimorphic cocrystallization of BS and BTF. In the first heating scan, PBTF showed obvious semi-crystalline properties, and its melting peak and cold crystallization peak appeared at 154 and 75.6 °C, respectively. PBSTFs copolyesters all had a single glass transition temperature, and T_g of copolyesters showed a rising trend with the increase of TDCA, indicating that the introduction of TDCA increased the rigidity of PBS and reduced the chain flexibility of PBS. For PBS, the glass transition temperature can not be observed under the second heating scan at the rate of 10 °C/min, meaning that the crystallization ability of PBS is very fast. Figure 6 shows TGA and DTG curves of PBS, PBTF, and PBSTFs in N_2. Table 3 summarizes the decomposition temperature at 5% weight loss ($T_{d,5\%}$) and

Table 3. $T_{d,5\%}$ and $T_{d, max}$ of PBS, PBTF, and PBSTFs determined by TGA.

Sample	$T_{d,5\%}$ [°C]	$T_{d, max}$ [°C]
PBS	349	394
PBSTF29	336	386
PBSTF48	339	385
PBSTF73	341	386
PBTF	351	385

the decomposition temperature at the maximum decomposition rate ($T_{d, max}$). All the synthesized polymers did not lose weight before 300 °C, indicating that the copolymers of PBS, PBTF, and PBSTFs had very good thermal stability. Significant weight loss occurs only when the temperature of the obtained polymer is greater than 380 °C, and the temperature is higher than 390 °C when the weight loss of the sample is 50%. $T_{d,5\%}$ and $T_{d, max}$ of PBS were 349, and 394 °C, respectively, and $T_{d,5\%}$ and $T_{d, max}$ of PBTF were 351 and 385 °C, respectively, which were similar to those reported in reference [18, 28].

3.3. Crystal structures of PBS, PBTF, and PBSTFs

The crystal structures of PBS, PBTF, and PBSTFs were further obtained by WAXD patterns in Figure 7. First, all samples were melted, and then they were put into liquid nitrogen to obtain amorphous samples. Finally, they were placed at 60 or 80 °C for 3 hours to obtain crystalline samples.

PBS, PBTF, and PBSTFs obtained are semi-crystalline polymers. The main diffraction peaks of PBS were observed at 19.6 and 25.9°. The weak peaks were observed at 25.9, 28.9, and 33.9°, which were
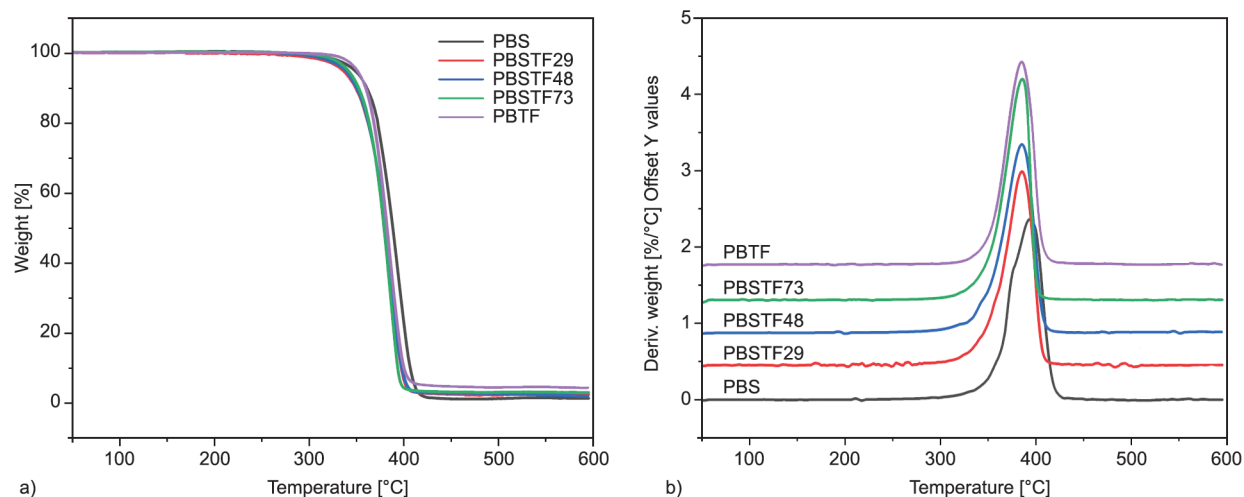

Figure 6. TGA (a) and DTG (b) curves of PBS, PBTF and PBSTFs under dynamic N_2 atmosphere.
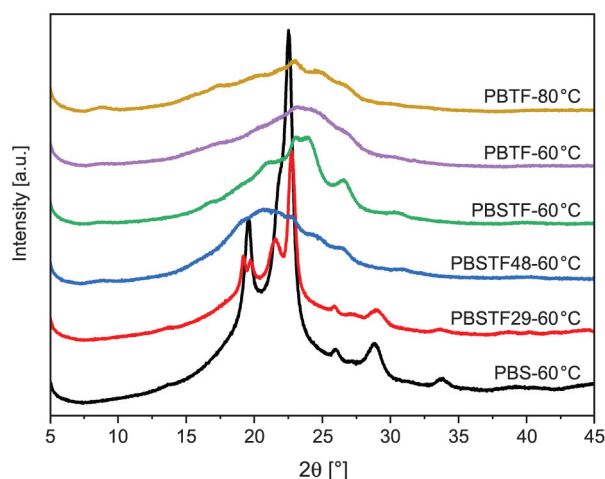
Figure 7. WAXD patterns of PBS, PBTF and PBSTFs co-polyester films annealed at 60 or 80 °C for 3 hours.

basically consistent with the reference [21, 33–35]. It can be known that these diffraction peaks were derived from α-crystal of PBS. The diffraction peaks of PBSTF29 are basically the same as those of PBS, which proves that PBSTF29 exhibits α-crystal of PBS. The diffraction peaks of PBSTF48 were the weakest. The diffraction peak of PBTF was lower than that of PBSTF73. The reason might be as follows: the crystallization ability of PBTF is worse than that of PBSTF73 at 60 °C because the glass transition temperature of PBTF is higher than that of PBSTF73. In order to obtain high crystallinity, PBTF was melted and then put into liquid nitrogen. Finally, PBTF was placed at 80 °C for 3 hours. The obtained PBTF showed obvious diffraction peaks. Compared with PBS, the intensity of the diffraction peak of PBSTF29 decreased because the chain mobility decreased due to the introduction of TDCA. When the content of TDCA is higher than 40%, the crystal

structures of PBSTF48, PBSTF73, and PBTF vary obviously. According to the literature [36], there are three crystal phases (α, β, and γ) for PBTF and the α-crystal phase is the most stable phase. Main diffraction peaks of PBTF annealed at 80 °C are located at 22.9 and 24.7°, indicating that the crystal is α-crystal phase.

3.4. Mechanical properties

The mechanical properties of the synthesized polyester were tested by Instron 3365 testing machine, including Young's modulus (E), tensile strength (σ_m), and elongation at break (ε_b). The data obtained are shown in Table 4. The mechanical properties of the material are mainly affected by the crystallinity and glass transition temperature of the sample. At the same time, in order to characterize the crystallinity of the tensile samples, the tensile samples were tested by WAXD (Figure 8). Figure 8 shows the stress-strain curves of the samples.

WAXD of the tensile samples shows that with the increase of TDCA, the intensity of the diffraction peaks gradually weakened. PBS and PBSTF29 showed similar sharp diffraction peaks, indicating that PBS and PBSTF29 had similar crystal structure and high crystallinity. With the increase of TDCA content,

Table 4. Young's modulus, tensile strength and elongation at break of PBS, PBTF and PBSTFs.

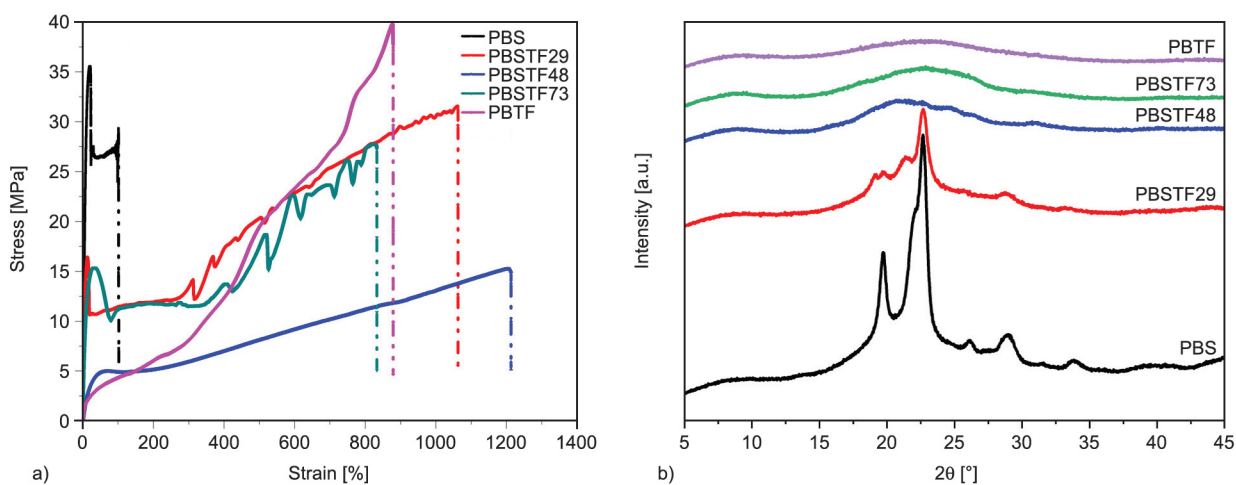| Sample	E [MPa]	σ_m [MPa]	ε_b [%]
PBS	448.0±13.0	35.2±1.5	124±23
PBSTF29	256.0±14.0	31.4±1.6	1060±60
PBSTF48	27.9±2.1	15.4±3.4	1160±280
PBSTF73	186.0±40.0	27.7±4.9	820±92
PBTF	7.2±0.7	38.0±3.4	863±51

Figure 8. (a) Representative stress–strain curves and (b) WAXD curves of PBS, PBTF and PBSTFs.

PBSTF48, PBSTF73, and PBTF showed wide diffraction peaks, indicating the crystallization ability of PBSTF48, PBSTF73, and PBTF was poor, and the tensile samples were basically amorphous.

The tensile properties of PBS (E = 448 MPa, σ_m = 35 MPa, ε_b = 124%) are similar to that of commercial PBS [37]. As can be seen from Table 4, with the increase of TDCA content, Young's modulus, tensile strength, and elongation at the break of PBSTFs first decreased and then increased. Compared with PBS, the tensile strength of PBSTF29 (31.4 MPa) decreased slightly, but the elongation at break (1060%) was significantly higher than that of PBS. Because PBS and PBSTF29 have high crystallinity, their yield strength is large (Figure 8). Young's modulus (256 MPa) of PBSTF29 is close to poly(butylene succinate-*co*-butylene adipate) [38], and poly(ε-caprolactone) [39], but higher than poly(butylene adipate-*co*-terephthalate) [40]. PBSTF48, PBSTF73, and PBTF are basically amorphous polymers. At the same time, the glass transition temperature is lower than 30 °C, which leads to their low modulus and high elongation at break. When the content of TDCA in the feed was 50%, the tensile strength of PBSTF48 (15.4 MPa) decreased significantly, and the elongation at break (1160%) increased slightly due to the lowest crystallinity. When the feed ratio of TDCA is less than or equal to 50%, the changes in Young's modulus and tensile strength are consistent with that of the crystallinity. It is proved that when the feed ratio of TDCA is less than or equal to 50%, the mechanical properties are mainly affected by the crystallinity. When the content of TDCA in the feed varied from 50 to 100%, tensile strength increased significantly, and the elongation at break increased slightly. PBSTF73 and PBTF are basically amorphous samples (Figure 8), meaning that the difference in tensile strength of PBSTF48, PBSTF73, and PBTF is not caused by different crystallinity. Compared with PBSTF48 and PBSTF73, PBTF has higher tensile strength, which is mainly due to the increase in glass transition temperature caused by the increase of TDCA.

In addition, in the tensile curves, the 'saw shape' phenomenon is the sign of fiber breakage in fiber-reinforced polymer composites. However, if the semicrystalline polymers can undergo strain-induced crystallization or orientation at the test temperature, the 'saw shape' phenomenon may also occur. In the literature [41], the 'saw shape' phenomenon of PBS has been explained in detail. Strain-induced crystallization or orientation will lead to an increase in stress. However, the occurrence of voids during neck propagation will lead to a sudden decrease in stress. Porosity and cavitation are the ultimate causes of the stress oscillation process. This phenomenon was also observed in the stress-strain curves of poly(butylene succinate-*co*-butylene carbonate) [3] and poly(butylene succinate-*co*-glycolate) [21].

3.5. Rheological properties

Since temperature is very important for the processing of polymers, the rheological properties can be seen as a function of the modulus and viscosity of the material versus temperature. The storage modulus represents the elasticity of the material, and the loss modulus represents the viscosity of the material. The rheological curves of PBS, PBTF, and PBSTFs are shown in Figure 9. For PBS, PBTF, and PBSTFs, the complex viscosity of the polymers gradually decreases with increasing temperature. Compared with PBS, PBSTF29 and PBSTF48 exhibited lower processing temperatures due to lower melting temperatures and glass transition temperatures. Storage modulus, loss modulus, and complex viscosity of the samples decreased with the increase in temperature. The decrease in the storage modulus of the samples indicates a decrease in the elasticity of the samples. Storage modulus and loss modulus of PBSTF29 and PBSTF48 are lower, indicating that the viscoelasticity of these two copolymers is not as good as the other samples. At 165 °C, storage modulus, loss modulus, and complex viscosity decreased and then increased with the increase of TDCA. When the content of BTF units exceeded 29%, storage modulus, loss modulus, and complex viscosity of the copolyesters became larger. Due to the stronger structural stability of BTF units, the copolyester is promoted to have better resistance to deformation. Meanwhile, due to the presence of a thiophene ring, the change of external force requires more time and energy to achieve the sliding of BTF units. Therefore, the higher the content of BTF units, the more pronounced the viscosity of the sample.

4. Conclusions

Novel aliphatic aromatic copolyesters were synthesized by direct esterification and polycondensation using TDCA, SA, and BDO as raw materials and TBT as a catalyst. Copolyesters have the desired
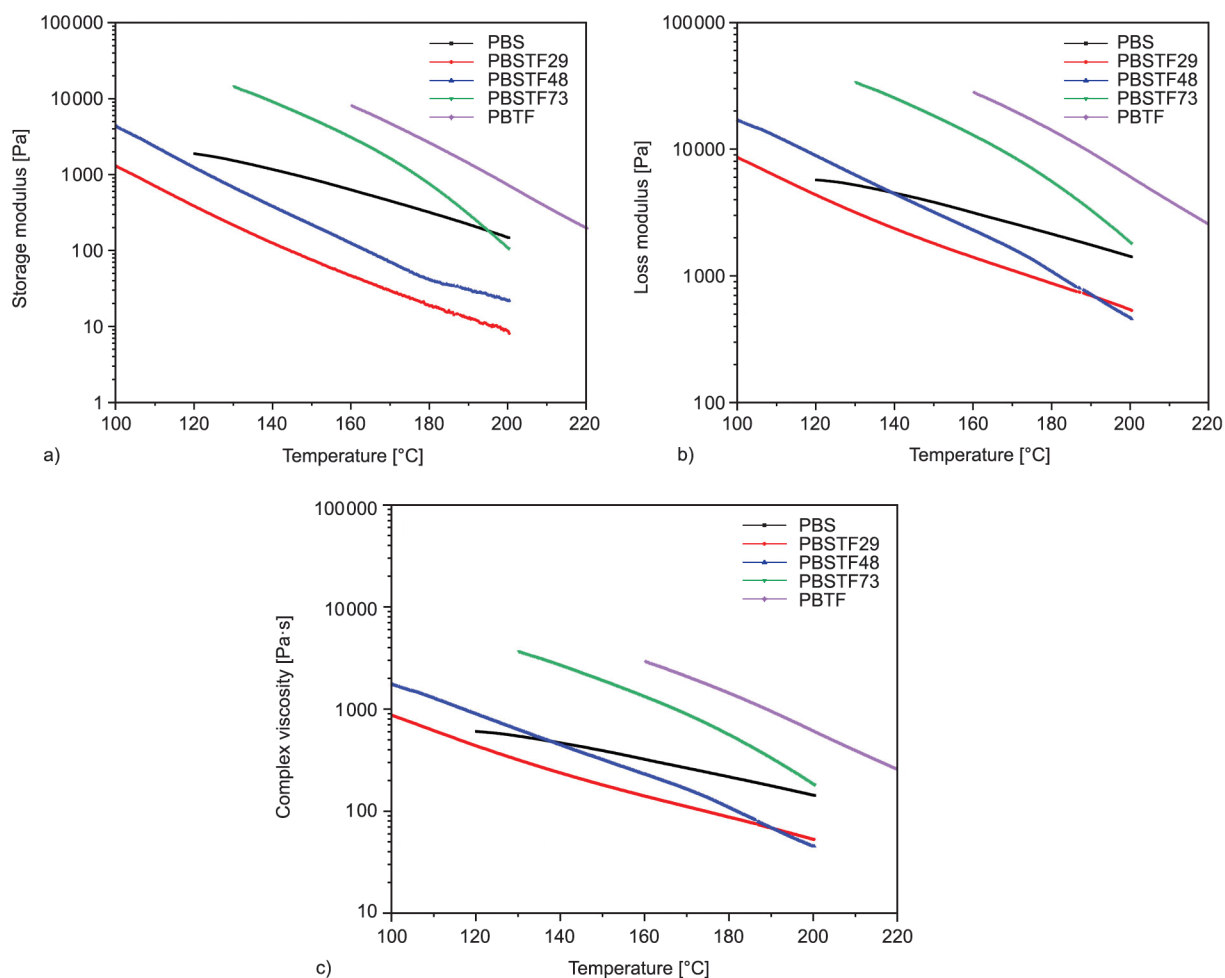
Figure 9. Rheological curves of PBS, PBTF and PBSTFs at different temperatures. a) Storage modulus, b) loss modulus, c) complex viscosity.

chemical structure, and the feed ratio of two diacid monomers controls the composition of the copolymers. They have excellent thermal stability, significant weight loss occurs after 380 °C, and no significant weight loss occurs before 300 °C. T_g increases continuously with the content of the BTF unit. With the addition of TDCA, the crystallinity and T_m of PBSTFs decreased, but with the further increase of TDCA content, T_m of BTF-rich PBSTFs increased. The tensile results show that except PBS, the elongation at break of other polyesters with good toughness remains in the range of 820–1160%. When the feed ratio of TDCA is less than or equal to 50%, the mechanical properties are mainly affected by the crystallinity. When the content of TDCA in feed varies from 50 to 100%, the mechanical properties are mainly affected by the glass transition temperature. Compared with PBS, PBSTF29 has better mechanical properties (tensile strength: 31.4 MPa, elongation at break: 1060%) and higher glass transition

temperature (–26.2 °C). Meanwhile, PBSTF29 has better processing properties. In summary, PBSTF29 is a kind of promising bio-based copolyester with better properties.

Acknowledgements

References

[1] Coombs J., Hall K.: Chemicals and polymers from biomass. Renewable Energy, **15**, 54–59 (1998).
https://doi.org/10.1016/S0960-1481(98)00136-0

[2] Rabnawaz M., Wyman I., Auras R., Cheng S.: A roadmap towards green packaging: The current status and future outlook for polyesters in the packaging industry. Green Chemistry, **19**, 4737–4753 (2017).
https://doi.org/10.1039/C7GC02521A

[3] Kim H., Jeon H., Shin G., Lee M., Jegal J., Hwang S. Y., Oh D. X., Koo J. M., Eom Y., Park J.: Biodegradable nanocomposite of poly(ester-*co*-carbonate) and cellulose nanocrystals for tough tear-resistant disposable bags. Green Chemistry, **23**, 2293–2299 (2021).
https://doi.org/10.1039/D0GC04072J

[4] Hurley R., Woodward J., Rothwell J. J.: Microplastic contamination of river beds significantly reduced by catchment-wide flooding. Nature Geoscience, **11**, 251–257 (2018).
https://doi.org/10.1038/s41561-018-0080-1

[5] Rillig M., Lehmann A.: Microplastic in terrestrial ecosystems. Science, **368**, 1430–1431 (2020).
https://doi.org/10.1126/science.abb5979

[6] Plichta A., Jaskulski T., Lisowska P., Macios K., Kundys A.: Elastic polyesters improved by ATRP as reactive epoxy-modifiers of PLA. Polymer, **72**, 307–316 (2015).
https://doi.org/10.1016/j.polymer.2015.03.055

[7] Guidotti G., Soccio M., Lotti N., Gazzano M., Siracusa V., Munari A.: Poly(propylene 2,5-thiophenedicarboxylate) *vs*. poly(propylene 2,5-furandicarboxylate): Two examples of high gas barrier bio-based polyesters. Polymers, **10**, 785 (2018).
https://doi.org/10.3390/polym10070785

[8] Mizuno S., Maeda T., Kanemura C., Hotta A.: Biodegradability, reprocessability, and mechanical properties of polybutylene succinate (PBS) photografted by hydrophilic or hydrophobic membranes. Polymer Degradation and Stability, **117**, 58–65 (2015).
https://doi.org/10.1016/j.polymdegradstab.2015.03.015

[9] Bin T., Qu J-P., Liu L-M., Feng Y-H., Hu S-X., Yin X-C.: Non-isothermal crystallization kinetics and dynamic mechanical thermal properties of poly(butylene succinate) composites reinforced with cotton stalk bast fibers. Thermochimica Acta, **525**, 141–149 (2011).
https://doi.org/10.1016/j.tca.2011.08.003

[10] Tang Y-R., Lin D-W., Gao Y., Xu J., Guo B-H.: Prominent nucleating effect of finely dispersed hydroxyl-functional hexagonal boron nitride on biodegradable poly(butylene succinate). Industrial and Engineering Chemistry Research, **53**, 4689–4696 (2014).
https://doi.org/10.1021/ie403915j

[11] Papageorgiou G. Z., Papageorgiou D. G., Chrissafis K., Bikiaris D., Will J., Hoppe A., Roether J. A., Boccaccini A. R.: Crystallization and melting behavior of poly(butylene succinate) nanocomposites containing silica-nanotubes and strontium hydroxyapatite nanorods. Industrial and Engineering Chemistry Research, **53**, 678–692 (2014).
https://doi.org/10.1021/ie403238u

[12] Song L., Qiu Z.: Influence of low multi-walled carbon nanotubes loadings on the crystallization behavior of biodegradable poly(butylene succinate) nanocomposites. Polymers for Advanced Technologies, **22**, 1642–1649 (2011).
https://doi.org/10.1002/pat.1652

[13] Liang Z., Pan P., Zhu B., Dong T., Inoue Y.: Mechanical and thermal properties of poly(butylene succinate)/plant fiber biodegradable composite. Journal of Applied Polymer Science, **115**, 3559–3567 (2010).
https://doi.org/10.1002/app.29848

[14] Liu L., Yu J., Cheng L., Qu W.: Mechanical properties of poly(butylene succinate) (PBS) biocomposites reinforced with surface modified jute fibre. Composites Part A: Applied Science and Manufacturing, **40**, 669–674 (2009).
https://doi.org/10.1016/j.compositesa.2009.03.002

[15] Lee S. M., Cho D., Park W. H., Lee S. G., Han S. O., Drzal L. T.: Novel silk/poly(butylene succinate) biocomposites: The effect of short fibre content on their mechanical and thermal properties. Composites Science and Technology, **65**, 647–657 (2005).
https://doi.org/10.1016/j.compscitech.2004.09.023

[16] Wang X., Yang H., Song L., Hu Y., Xing W., Lu H.: Morphology, mechanical and thermal properties of graphene-reinforced poly(butylene succinate) nanocomposites. Composites Science and Technology, **72**, 1–6 (2011).
https://doi.org/10.1016/j.compscitech.2011.05.007

[17] Wu L., Mincheva R., Xu Y., Raquez J-M., Dubois P.: High molecular weight poly(butylene succinate-*co*-butylene furandicarboxylate) copolyesters: From catalyzed polycondensation reaction to thermomechanical properties. Biomacromolecules, **13**, 2973-2981 (2012).
https://doi.org/10.1021/bm301044f

[18] Luo S., Li F., Yu J.: The thermal, mechanical and viscoelastic properties of poly(butylene succinate-*co*-terephthalate) (PBST) copolyesters with high content of BT units. Journal of Polymer Research, **18**, 393–400 (2011).
https://doi.org/10.1007/s10965-010-9429-x

[19] Peng S., Wu L., Li B-G., Dubois P.: Hydrolytic and compost degradation of biobased PBSF and PBAF copolyesters with 40–60 mol% BF unit. Polymer Degradation and Stability, **146**, 223–228 (2017).
https://doi.org/10.1016/j.polymdegradstab.2017.07.016

[20] Hong G., Cheng H., Zhang S., Rojas O. J.: Mussel-inspired reinforcement of a biodegradable aliphatic polyester with bamboo fibers. Journal of Cleaner Production, **296**, 126587 (2021).
https://doi.org/10.1016/j.jclepro.2021.126587

[21] Hu H., Li J., Tian Y., Chen C., Li F., Ying W. B., Zhang R., Zhu J.: Experimental and theoretical study on glycolic acid provided fast bio/seawater-degradable poly(butylene succinate-*co*-glycolate). ACS Sustainable Chemistry and Engineering, **9**, 3850–3859 (2021).
https://doi.org/10.1021/acssuschemeng.0c08939

[22] Duan R-T., He Q-X., Dong X., Li D-F., Wang X-L., Wang Y-Z.: Renewable sugar-based diols with different rigid structure: Comparable investigation on improving poly(butylene succinate) performance. ACS Sustainable Chemistry and Engineering, **4**, 350–362 (2016).
https://doi.org/10.1021/acssuschemeng.5b01335

[23] Tsanaktsis V., Papageorgiou D. G., Exarhopoulos S., Bikiaris D. N., Papageorgiou G. Z.: Crystallization and polymorphism of poly(ethylene furanoate). Crystal Growth and Design, **15**, 5505–5512 (2015).
https://doi.org/10.1021/acs.cgd.5b01136

[24] Papageorgiou G. Z., Papageorgiou D. G., Tsanaktsis V., Bikiaris D. N.: Synthesis of the bio-based polyester poly(propylene 2,5-furan dicarboxylate). Comparison of thermal behavior and solid state structure with its terephthalate and naphthalate homologues. Polymer, **62**, 28–38 (2015).
https://doi.org/10.1016/j.polymer.2015.01.080

[25] Papageorgiou G. Z., Tsanaktsis V., Papageorgiou D. G., Exarhopoulos S., Papageorgiou M., Bikiaris D. N.: Evaluation of polyesters from renewable resources as alternatives to the current fossil-based polymers. Phase transitions of poly(butylene 2,5-furan-dicarboxylate). Polymer, **55**, 3846–3858 (2014).
https://doi.org/10.1016/j.polymer.2014.06.025

[26] Zhou W., Wang X., Yang B., Xu Y., Zhang W., Zhang Y., Ji J.: Synthesis, physical properties and enzymatic degradation of bio-based poly(butylene adipate-*co*-butylene furandicarboxylate) copolyesters. Polymer Degradation and Stability, **98**, 2177–2183 (2013).
https://doi.org/10.1016/j.polymdegradstab.2013.08.025

[27] Wang G., Hao X., Jiang M., Wang R., Liang Y., Zhou G.: Partially bio-based copolyesters poly(ethylene 2,5-thiophenedicarboxylate-*co*-ethylene terephthalate): Synthesis and properties. Polymer Degradation and Stability, **181**, 109369 (2020).
https://doi.org/10.1016/j.polymdegradstab.2020.109369

[28] Guidotti G., Gigli M., Soccio M., Lotti N., Gazzano M., Siracusa V., Munari A.: Poly(butylene 2,5-thiophenedicarboxylate): An added value to the class of high gas barrier biopolyesters. Polymers, **10**, 167 (2018).
https://doi.org/10.3390/polym10020167

[29] Wang G., Jiang M., Zhang Q., Wang R., Liang Q., Zhou G.: New bio-based copolyesters poly(trimethylene 2,5-thiophenedicarboxylate-*co*-trimethylene terephthalate): Synthesis, crystallization behavior, thermal and mechanical properties. Polymer, **173**, 27–33 (2019).
https://doi.org/10.1016/j.polymer.2019.04.024

[30] Hu L., Wu L., Song F., Li B-G.: Kinetics and modeling of melt polycondensation for synthesis of poly[(butylene succinate)-*co*-(butylene terephthalate)], 1 – esterification. Macromolecular Reaction Engineering, **4**, 621–632 (2010).
https://doi.org/10.1002/mren.201000021

[31] Chen X., Chen W., Zhu G., Huang F., Zhang J.: Synthesis, ^{1}H-NMR characterization, and biodegradation behavior of aliphatic–aromatic random copolyester. Journal of Applied Polymer Science, **104**, 2643–2649 (2007).
https://doi.org/10.1002/app.25611

[32] Witt U., Müller R-J., Deckwer W-D.: Studies on sequence distribution of aliphatic/aromatic copolyesters by high-resolution ^{13}C nuclear magnetic resonance spectroscopy for evaluation of biodegradability. Macromolecular Chemistry and Physics, **197**, 1525–1535 (1996).
https://doi.org/10.1002/macp.1996.021970428

[33] Liu G., Zheng L., Zhang X., Li C., Jiang S., Wang D.: Reversible lamellar thickening induced by crystal transition in poly(butylene succinate). Macromolecules, **45**, 5487–5493 (2012).
https://doi.org/10.1021/ma300530a

[34] Qiu Z., Yang W.: Crystallization kinetics and morphology of poly(butylene succinate)/poly(vinyl phenol) blend. Polymer, **47**, 6429–6437 (2006).
https://doi.org/10.1016/j.polymer.2006.07.001

[35] Platnieks O., Gaidukovs S., Neibolts N., Barkane A., Gaidukova G., Thakur V. K.: Poly(butylene succinate) and graphene nanoplatelet–based sustainable functional nanocomposite materials: Structure-properties relationship. Materials Today Chemistry, **18**, 100351 (2020).
https://doi.org/10.1016/j.mtchem.2020.100351

[36] Guidotti G., Gigli M., Soccio M., Lotti N., Gazzano M., Siracusa V., Munari A.: Ordered structures of poly(butylene 2,5-thiophenedicarboxylate) and their impact on material functional properties. European Polymer Journal, **106**, 284–290 (2018).
https://doi.org/10.1016/j.eurpolymj.2018.07.027

[37] Xu J., Guo B-H.: Poly(butylene succinate) and its copolymers: Research, development and industrialization. Biotechnology Journal, **5**, 1149–1163 (2010).
https://doi.org/10.1002/biot.201000136

[38] Nofar M., Tabatabaei A., Sojoudiasli H., Park C. B., Carreau P. J., Heuzey M-C., Kamal M. R.: Mechanical and bead foaming behavior of PLA-PBAT and PLA-PBSA blends with different morphologies. European Polymer Journal, **90**, 231–244 (2017).
https://doi.org/10.1016/j.eurpolymj.2017.03.031

[39] Hua L., Chen Q., Yin J., Zhang C., Wang X., Yin J., Feng X., Yang J.: Fabrication and physical properties of poly(ε-caprolactone)/modified graphene nanocomposite. Macromolecular Materials and Engineering, **302**, 1600328 (2017).
https://doi.org/10.1002/mame.201600328

[40] Liu W., Liu T., Liu H., Xin J., Zhang J., Muhidinov Z. K., Liu L.: Properties of poly(butylene adipate-*co*-terephthalate) and sunflower head residue biocomposites. Journal of Applied Polymer Science, **134**, 44644 (2017).
https://doi.org/10.1002/app.44644

[41] Wan C., Heeley E. L., Zhou Y., Wang S., Cafolla C. T., Crabb E. M., Hughes D. J.: Stress-oscillation behaviour of semi-crystalline polymers: The case of poly(butylene succinate). Soft Matter, **14**, 9175–9184 (2018).
https://doi.org/10.1039/c8sm01889h